



# Siloxane-modified bacterial cellulose as a promising platform for cell culture

Amanda Maria Claro · Nayara Cavichioli Do Amaral · Vitória Maria Medalha Colturato · Nadia Andrade Aleixo · Robert Paiva · Sandra Andrea Cruz · Gustavo Claro Monteiro · Gustavo Senra Gonçalves De Carvalho · Flávia Aparecida Resende Nogueira · Elenice Deffune · Mônica Rosas da Costa Iemma · Hernane da Silva Barud

Received: 14 February 2022 / Accepted: 25 September 2022 / Published online: 16 October 2022  
© The Author(s), under exclusive licence to Springer Nature B.V. 2022

**Abstract** Cellulose is a versatile tunable material that finds application in the biomedical field as substrate for cell culture. However, few studies have been done to explore the use of bacterial cellulose (BC), a naturally occurring nanofibrillar material with distinct properties, as a platform to produce such device. In the present work, BC membranes have been functionalized with thiol functional group (SH) through silanization reaction with (3-mercaptopropyl)

trimethoxysilane (MPTMS) under different conditions, in order to obtain a platform with improved cell adhesion. The efficiency of BC surface modification with MPTMS was evaluated by using acid and base catalyzed reactions, and two different drying methods: at room temperature of 28 °C and at 120 °C as curing temperature. The results of the set of analyses performed—ATR-FTIR, TGA, elemental analysis, <sup>13</sup>C NMR, contact angle and SEM—indicate that BC surface functionalization was efficient, regardless the drying process. The MPTMS-modified platforms exhibited sulfur content of 3–5 times higher than native BC. The performed biological assay with fibroblast GM07492 human cells revealed that adhesion of cells to the BC surface depends not only on the functional group present at the matrix but also on surface wettability.

**Supplementary Information** The online version contains supplementary material available at <https://doi.org/10.1007/s10570-022-04872-4>.

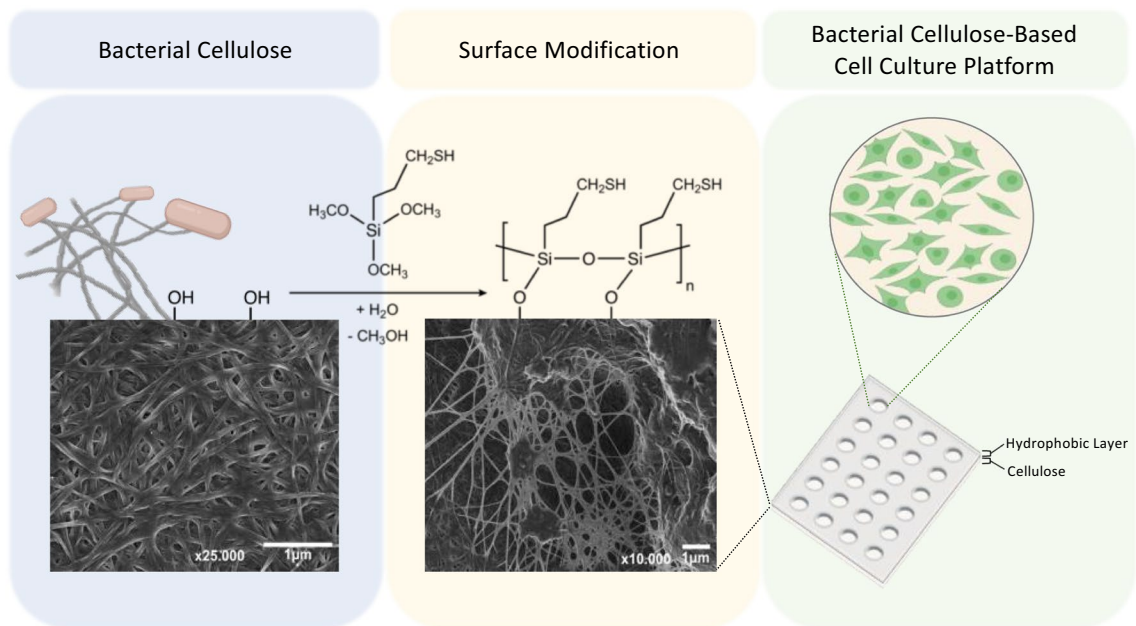
A. M. Claro · N. C. Do Amaral · V. M. M. Colturato · N. A. Aleixo · G. S. G. De Carvalho · F. A. R. Nogueira · M. R. d. Iemma · H. d. Barud (✉)  
University of Araraquara - UNIARA, Rua Carlos Gomes 1217, Araraquara, SP 14801-340, Brazil  
e-mail: hernane.barud@gmail.com

R. Paiva · S. A. Cruz  
Department of Chemistry, Federal University of São Carlos, P.O. Box 676, São Carlos, SP 13560-970, Brazil

G. C. Monteiro  
TechMiP Análises e Soluções Inteligentes LTDA,  
Av. Jorge Fernandes de Mattos 311, Araraquara,  
SP 14808-162, Brazil

E. Deffune  
Medical School, Sao Paulo State University Julio de Mesquita Filho, Av. Prof. Mário Rubens Guimarães Montenegro, s/n - UNESP - Campus de Botucatu,  
Botucatu 18618-687, Brazil

## Graphical abstract



Schematic illustration of a siloxane-modified bacterial cellulose as platform for cell culture.

**Keywords** Bacterial cellulose · Siloxane · Mercapto · Platform · Cell culture

## Introduction

Cell culture has been traditionally used to allow the maintenance of living cells, particularly in pharmacological screening for the purpose of pre-clinical drug discovery. More recently, the cultivation of cells on platforms has also been used to mimic a variety of living tissues for the development of disease models, in cell cryopreservation, and tissue engineering, technologies that are growing in importance at a faster pace (Ng et al. 2016; Lantigua et al. 2017). Many types of natural and synthetic polymers that support cell adhesion and spreading have been used in the production of cell culture platforms (Ng et al. 2016; Mirbagheri et al. 2019).

Recently, cellulosic substrates have been successfully used in the production of 3D cell culture

systems by stacking paper sheets. The advantages of using cellulose-based cell culture platforms include its biocompatibility to human cells, as it is a substrate coming from a sustainable natural source and its biodegradability by many microorganisms (Ng et al. 2016). Particularly, bacterial cellulose (BC) is a pure nanocellulose not toxic to cells that is produced by some non-pathogenic bacteria in the form of a gelatinous pellicle under static cultivation. When it dries, this membrane turns into a paper-like membrane of pure cellulose whose application is very promising in medical and biomedical fields (de Oliveira Barud et al. 2016; Urbina et al. 2021). The remarkable three-dimensional (3D) open fibril network nanostructure of BC retains water and favors the transportation of nutrients which are advantageous for cell ingrowth. Furthermore, BC thickness and porosity (92% for freeze-dried membranes and 65% for hot air-dried membranes) can be tailored to requirements (Tang et al. 2009).

3D cell culture fabricated by multilayered paper construct allows proper oxygen and nutrient diffusion favoring cell growth, proliferation, and

differentiation. Paper-based platform design and cell containing zones can be customized using wax printing. The hydrophobic coating is intended to isolate the channels and to provide mechanical support. The great advantage of using cell culture platforms refers to the possibility of analyzing cellular behavior under the most diverse circumstances (including drugs/biomolecules administration, nutrients presence and gas gradient) without manipulating living organisms (Ng et al. 2016; Tibbitt and Anseth 2009; Edmondson et al. 2014).

BC is a natural polymeric substrate that lacks biological recognition elements, requiring manipulation to improve cell adhesiveness onto its surface (Ng et al. 2016; Mirbagheri et al. 2019; de Oliveira Barud et al. 2016). Several modification methods of BC have been investigated to optimize interactions between this biomaterial and different cell lines, including chemical surface which is able to change properties such as permeability, wettability, and porosity (de Oliveira Barud et al. 2016). From this perspective, Taokaew et al. (2015) investigated the effect of functionalizing BC surface by grafting amine ( $\text{NH}_2$ ) and methyl ( $\text{CH}_3$ ) terminated organosilanes (3-aminopropyl)triethoxysilane (APTES) and octadecyltrichlorosilane (OTS) on human dermal fibroblasts adhesion. The surface treatment with APTES has been shown to improve cell attachment and spreading (70–80% area coverage by cells) compared to the unmodified BC surface, while the opposite result (<5% area coverage) was observed for the OTS-functionalized BC surface.

In this study, BC surface was functionalized with thiol group (SH) by silanization using two different chemical methods and the influence on the adhesion of normal human lung fibroblasts was evaluated. For the best of our knowledge (3-mercaptopropyl)trimethoxysilane (MPTMS) functionalized BC was not yet explored for this purpose. The chemical grafting and the reaction mechanism of the silane surface modification is shown in the Supplementary Material.

## Experimental section

### Bacterial cellulose production

The BC membranes were gently provided by the NEXFILL company (Seven Indústria de Produtos Biotecnológico Ltda) from Brazil. The cultivation of the bacterium *Komagataeibacter xylinus* was carried out in 30 cm × 50 cm shallow trays at 28 °C for 96 h. The culture medium has the following basic composition: 2% glucose (w/v), 0.5% peptone (w/v), 0.5% yeast extract (w/v), 0.27% disodium phosphate (w/v), and 0.115% citric acid monohydrate (w/v). The highly hydrated BC sheets were treated with 1 M NaOH solution at 70 °C to remove the bacteria. The commercially dry membranes were approximately 0.02 mm thick.

### Preparation of modified BC platforms

Two methodologies were used for the BC surface functionalization with the thiol group using MPTMS. The first method comprises acid-catalyzed reaction in aqueous solution according to the conditions reported by Beaumont et al. (2018). The second method consists of a weak base-catalyzed reaction in ethanol:water (10:1; v/v) (Lu et al. 2012; Do Amaral et al. 2019).

#### Method 1—Silanization catalyzed by acid (CA)

The BC dry membranes were cut into pieces of 1 cm<sup>2</sup> and 0.25 g of the prepared material was added to a falcon tube. The membranes were placed in contact with the solvent (water) for 5 min. A catalytic amount of 0.5 M hydrochloric acid was added to the tube, followed by the addition of MPTMS to reach the final concentration of 0.043 mmolL<sup>-1</sup>. The system was kept under orbital stirring at 25 °C for 30 min. Then, 0.5 M sodium hydroxide was added to the tube and it was kept under stirring for further 3 h. Finally, the membranes were removed from the solution and washed with water and acetone to remove reaction residues. The platforms were dried at 28 °C (BC-SH CA dried at 28 °C) and at 120 °C (BC-SH CA dried at 120 °C) for 5 h.

## Method 2—Silanization catalyzed by base (CB)

0.25 g of 1 cm<sup>2</sup> BC dry membranes was added to a falcon tube. The membranes were placed in contact with the solvent (ethanol–water solution) for 5 min. Ammonium hydroxide was added to the tube, followed by the addition of MPTMS to reach the final concentration of 0.164 mmolmL<sup>-1</sup>. The system was kept under orbital stirring at 25 °C for 15 h. Finally, the membranes were removed from the solution and washed with water and acetone to remove reaction residues. The BC platforms were dried at 28 °C (BC-SH CB dried at 28 °C) and at 120 °C (BC-SH CB dried at 120 °C) for 5 h.

## Biological assays

To assess cellular adhesion to the surface of the produced materials, cell viability tests were performed by fluorescence method by resazurin reduction (Pagé et al. 1993). A total of three replicates of the experiment were performed. Normal human lung fibroblast GM07492 cells were cultured in DMEM medium (Dulbecco's Modified Eagle's Medium) supplemented with 10% fetal bovine serum and antibiotic solution and incubated in a humid chamber at 37 °C in an atmosphere of 5% CO<sub>2</sub>. Finally, the cells were disadhered by trypsin treatment. After centrifugation the dead cells were removed and counted by trypan blue method using a Neubauer counting chamber.

Triplicate wells of a 96-well plate were used for the cell viability assay in the following configuration: membrane, cells, membrane+cells. Cell suspension was seeded (1.5 × 10<sup>4</sup> cells/well) and 100 µl of PBS was added to the wells. The plate was incubated at 37 °C for 24 h. After the incubation, the medium was removed and the resazurin solution 10% (v/v) was added to each well. The plate was incubated for 4 h at 37 °C and the fluorescence of the well solution was measured using a microplate reader. The wells were washed with PBS solution to perform the cell viability assay within 48 h on the same well plate. Then, 100 µL of supplemented DMEM medium was added to the wells and the well plate was incubated for more 24 h (48 h total). Finally, 100 µL of resazurin solution was added to the wells and fluorescence was measured after 4 h of incubation at 37 °C.

Excitation and emission filters at 530 nm and 590 nm were used for the fluorescence assay and the measurements were performed in a Cytation microplate reader from Biotek®.

## Characterization and statistical analysis

### Structural characterization

#### *Thermogravimetric analysis*

The thermal properties of the platforms were determined by Thermogravimetric Analysis (TGA) and Derived Thermogravimetry (DTG). TGA/DTG curves were obtained on a TA Instruments SDT Q600 under the following conditions: synthetic air atmosphere with continuous flow of 100 mL/min and heating rate of 10 °C/min over temperature range of 30–600 °C using a sample mass of about 5 mg. Alumina pan was used as reference.

#### *Elemental analysis*

Total carbon, hydrogen, nitrogen and sulfur were determined by dry combustion in a 2400 Series II CHNS elemental analyzer from Perkin Elmer.

#### *Solid State NMR of the <sup>13</sup>C nucleus*

Solid state <sup>13</sup>C NMR spectra were obtained at 7.04 T on a Bruker Avance III HD 300 spectrometer operating at a Larmor frequency of 75.00 MHz. The analyzes were acquired using a 4 mm MAS probe in ZrO<sub>2</sub> rotors (and Kel-F covers). The measurements were carried out at a frequency of 9000 Hz, with a relaxation time of 1 s and a pulse of 90° of 2.6 µs using magical spin-angle, and cross-polarization. The chemical shifts were indirectly standardized through a sample of glycine, with carbonyl sign at 176.00 ppm in relation to the TMS which is the primary standard.

**Table 1** Parameters of tension surface, dispersive and polar components for probe liquids, water and diiodomethane

Liquids	$\gamma_L$ (mN/m)	$\gamma_L^d$ (mN/m)	$\gamma_L^p$ (mN/m)
Water	72.8	21.8	51.0
Diiodomethane	50.8	50.8	0

## Surface characterization

### Vibrational spectroscopy in the infrared region

The BC platforms were structurally characterized by Attenuated Total Reflectance Fourier Transform Infrared Spectroscopy (ATR-FTIR). Infrared spectra were obtained on a Thermo Scientific NICOLET IS5 spectrometer with iD3 ATR transmission module with germanium crystal under the following conditions: 32 background scans, 32 sample analysis scans,  $2\text{ cm}^{-1}$  resolution and absorption range between  $4000$  and  $650\text{ cm}^{-1}$ .

### Contact angle

The surface behavior of the platforms was analyzed by contact angle in a Ramé-Hart 260-F4 Series-DROPimage Advanced v2.7 goniometer by the sessile drop method using water and diiodomethane as probe liquids which exhibit different polarity characteristics. The surface tension was calculated by using the Eq. 1 proposed by Wu (1971) and the parameters

of the probe liquids is described in Table 1. Equation 1 describes the calculation of surface tension for low energy surface solid materials.

$$\gamma_{LV}(1 + \cos \theta) = 4 \left[ \frac{\gamma_{SV}^D * \gamma_{LV}^D}{\gamma_{SV}^D + \gamma_{LV}^D} + \frac{\gamma_{SV}^P * \gamma_{LV}^P}{\gamma_{SV}^P + \gamma_{LV}^P} \right] \quad (1)$$

where  $\gamma_L$  is the tension of the liquid probe,  $\gamma_L^d$  and  $\gamma_L^p$  are the dispersive and polar components of the liquid, and  $\gamma_S^d$  and  $\gamma_S^p$  are the dispersive and polar components of the solid, respectively. The sum of the polar and dispersive components of the solid results on its surface tension.

### Scanning electron microscopy

The morphological characterization of the platforms was carried out using a Jeol JSM 7500F Field Emission Gun Scanning Electron Microscope (FEG-SEM). The samples were held in a brass stub and covered with a thin layer of carbon (approximately 5 nm thick) in a Bal-Tec SCD 050 Sputter Coater.

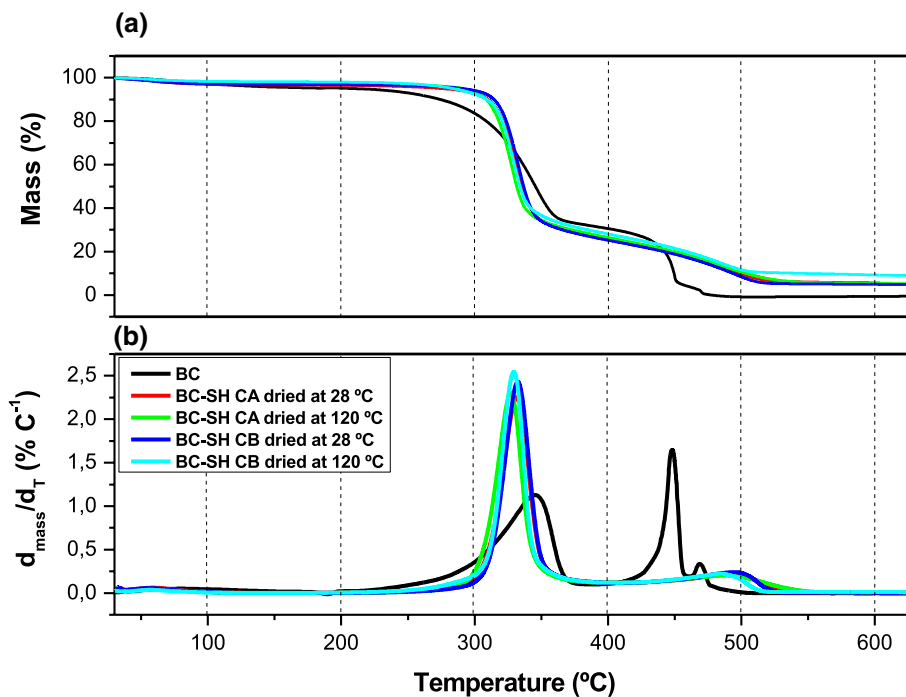


**Fig. 1** TG thermograms and differential thermogram of the BC-based platforms

**Table 2** Parameters obtained by TGA/DTG for the BC-based platforms

Sample	Water mass loss (%)	Mass loss 1st event (%)	Mass loss 2st event (%)	T <sub>i</sub> (5%)	T <sub>lmax</sub>	T <sub>2max</sub>	AT (T <sub>lmax</sub> –T <sub>i</sub> )
BC	5	60	35	203	345	448	142
BC-SH CA dried at 28 °C	3	69	17	276	331	497	55
BC-SH CA dried at 120 °C	2	68	17	291	327	488	36
BC-SH CB dried at 28 °C	2	69	17	290	332	494	42
BC-SH CB dried at 120 °C	1	68	15	282	328	481	46

### Statistical analysis

Statistical analysis was performed in GraphPad Prism software. Data resulting from the experiments were subjected to Student's t-test for comparison between pairs of groups (24 h and 48 h of cell incubation). Confidence level of 95% was selected and the cell viability of control after 24 h was assumed as 100%.

### Results and discussion

TGA was used to investigate the thermal and degradation properties of the prepared platforms; TGA thermograms and differential thermograms are shown in Fig. 1. In this work, the initial mass loss temperature (T<sub>i</sub>) was considered as the temperature on which the sample loses 5% of its mass. The mass loss of the samples occurs in two steps (200–500 °C) and relates to cellulose depolymerization and decomposition (de Oliveira Barud et al. 2015). These processes were determined by the peak of the first derivative of the curve of mass loss as a function of temperature, that is, by the maximum speed mass loss temperature, and named as T<sub>lmax</sub> and T<sub>2max</sub>. The difference between T<sub>lmax</sub> and T<sub>i</sub> (ΔT) is related to the mass loss kinetics. That is, the larger the ΔT value, the slower is the release of

the volatiles during the degradation process (Fitroni et al. 2015).

For BC, the absence of carbonaceous char residue at 600 °C is a clear indication that the material is pure. The final residual mass found for the modified BC-based platforms (5.6–9.3%) is attributed to the MPTMS grafted onto the cellulosic fibers. Furthermore, those platforms have exhibited a lower percentage of water loss adsorbed to the surface of the material compared to native BC. Table 2 presents the data extracted from the thermogram curves.

The modification of BC significantly increases T<sub>i</sub> values. Silanization takes place on the BC surface, in other words, silanol reacts with the hydroxyl group of BC resulting in the formation of strong covalent bonds (Supplementary Material). This modification acts as a barrier making gas diffusion difficult, that is, the volatiles output and the synthetic air input. However, an interesting behavior was noticed. The kinetics of the degradation (ΔT) for modified BC-based platform shows that the mass loss evolution is faster because of the presence of silane. As described in the literature (Quang Khieu et al. 2017), the temperature of silane decomposition can change according to its synthesis precursor. However, for silanization using MPTMS, degradation is described to occur at about 300 °C. For the BC-modified ones, a decrease in T<sub>lmax</sub> was observed probably caused by the silane decomposition that interferes in this process.

**Table 3** CHNS content of the BC-based platforms

Sample	Carbon (%)	Hydrogen (%)	Nitrogen (%)	Sulfur (%)
BC	42.45	5.75	0.87	1.04
BC-SH CA dried at 28 °C	40.46	6.46	0.96	5.47
BC-SH CA dried at 120 °C	41.79	6.50	1.16	3.38
BC-SH CB dried at 28 °C	40.16	6.26	0.91	3.73
BC-SH CB dried at 120 °C	41.24	6.39	1.03	3.93



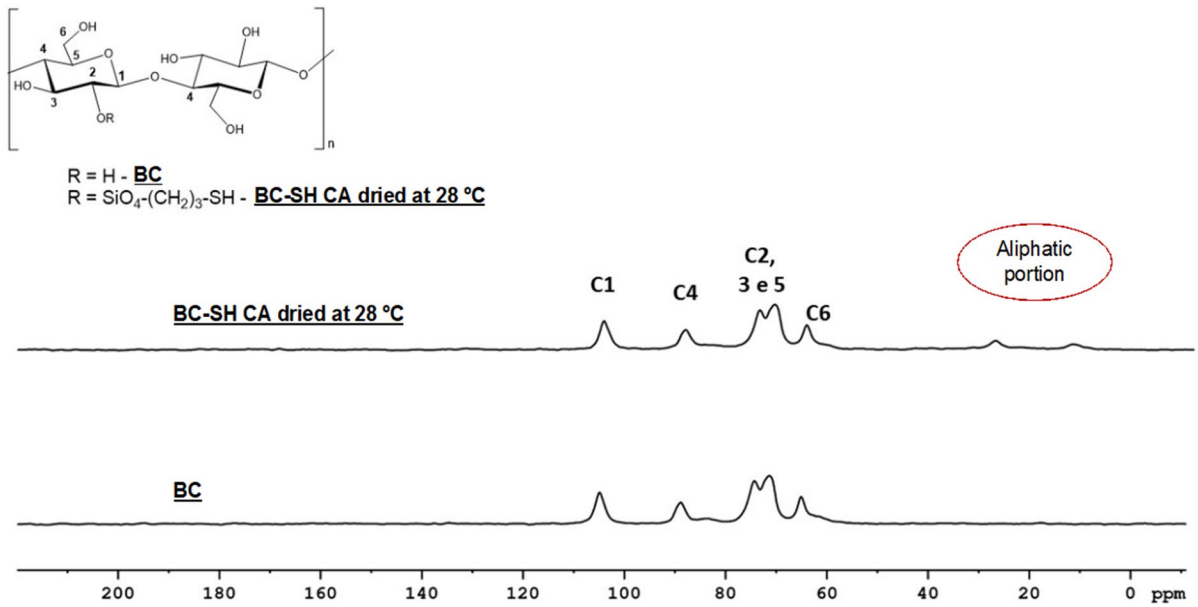


**Fig. 2** <sup>13</sup>C NMR spectra of pristine BC and BC-SH CA dried at 28 °C

**Fig. 3** FTIR spectra of the BC-based platforms

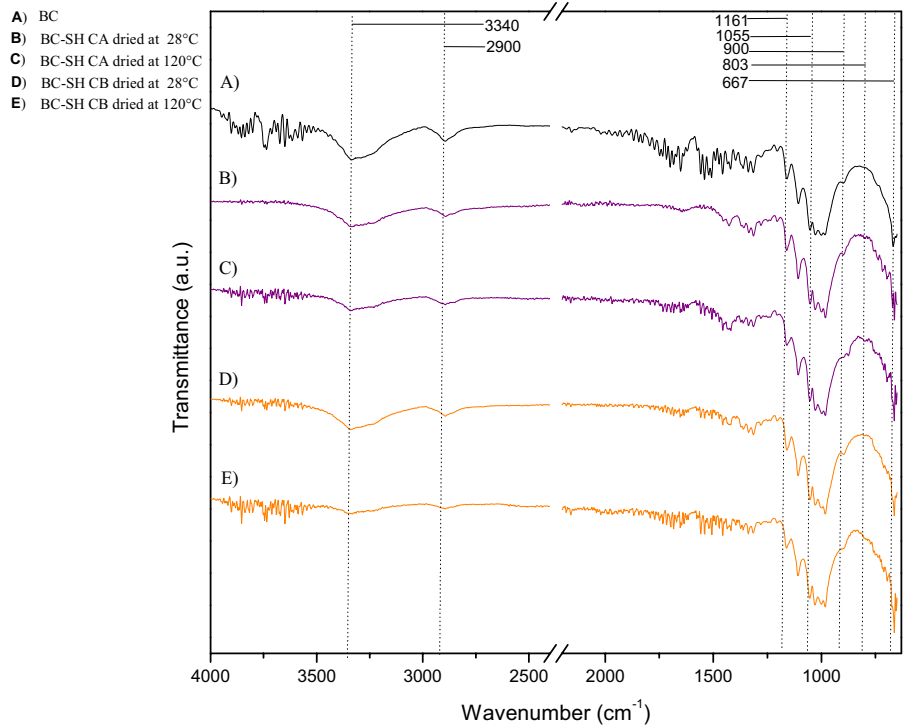


Table 3 provides the elemental analysis data. The sulfur (S) percentage associated with the modified BC-based platforms was 3–5 times compared to

pristine BC, demonstrating the effectiveness of the applied methodologies. Similar CHNS results have been previously published for BC and BC modified

with MPTMS under basic conditions (Do Amaral et al. 2019).

Figure 2 shows the  $^{13}\text{C}$  NMR spectra of pristine BC and BC-SH CA dried at 28 °C as a representative sample to testify the modification once it had exhibited the highest sulfur percentage according to the previous analysis. It is possible to observe in the spectra the signals related to the carbon atoms of carbohydrate portion of the cellulose structure. More specifically, the signal in the region of  $\delta$  105 ppm refers to carbon C1, the signal in  $\delta$  89 ppm refers to carbon C4. The signals in the region between  $\delta$  76–73 ppm refers to carbons C2, C3 and C5 and the signal in  $\delta$  65 ppm refers to carbon C6 (Kono et al. 2002; Daicho et al. 2020). Carbon atoms signals related to the aliphatic chains inserted onto BC are seen at  $\delta$  12.8 and 28.0 ppm. Furthermore, it is possible to observe signals in the region of  $\delta$  60 ppm associated with the methylene carbons of Si–OCH<sub>2</sub>R group which also indicates the incorporation of the aliphatic chains in the carbohydrate portion of the platform (Monteiro et al. 2021). These data strongly suggest that BC-SH CA dried at 28 °C has been modified.

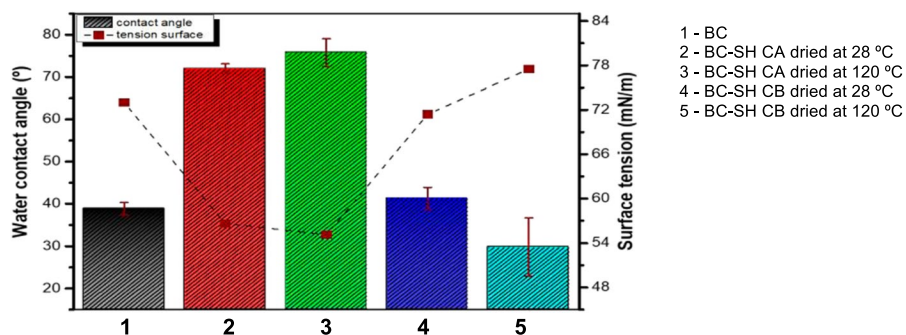
The infrared spectra of the materials are shown in Fig. 3. The spectra of the modified BC platforms (BC-SH CA dried at 28 °C, BC-SH CA dried at 120 °C, BC-SH CB dried at 28 °C, BC-SH CB dried at 120 °C) show similarity in band profile compared to native BC platform (BC) due to cellulose vibrational modes. The weak band at 900  $\text{cm}^{-1}$  is attributed to vibrational modes of the C–O–C  $\beta$  (1  $\rightarrow$ 4) glycosidic bonds between glucose units and a band at 1,055  $\text{cm}^{-1}$  is assigned to the C–O stretch of primary alcohol. A band at 1161  $\text{cm}^{-1}$  is attributed to C–O–C asymmetric vibrations of the pyranose ring of glucose. The band at 2900  $\text{cm}^{-1}$  is attributed to C–H and CH<sub>2</sub> stretching modes and the band at 3340  $\text{cm}^{-1}$

is assigned to O–H stretching of adsorbed water molecules on cellulose surface (De Salvi et al. 2012). For the modified BC-based platforms, bands related to Si–O stretching modes were not observed in the region of 1100–1200  $\text{cm}^{-1}$  due to the bands overlapping associated with the C–O–C vibrations of cellulose (Frone et al. 2018). However, the bands between 3000 and 3600  $\text{cm}^{-1}$  attributed to O–H stretching are less intense for the modified platforms compared to pristine BC platform. This might be explained by the decrease in the amount of free hydroxyl groups on the cellulose surface caused by the chemical treatment where its available O–H groups react with the MPTMS counterpart being replaced by a distinct covalent bond (O–Si) (Robles et al. 2018).

Figure 4 shows the water contact angle results and the change in surface tension values before and after the modification of the native BC platform by silane-grafting under acidic and basic conditions and thermal treatment. In the light of the results, the chemical treatment had significantly modified the surface properties of the BC platforms that underwent acidic conditions, with a considerable increase on their surface hydrophobicity. The modified platforms produced under basic conditions had maintained its hydrophilic character. However, it is observed that the thermal treatment had impacted the wetting behavior of the platforms, especially for those which had underwent basic conditions.

Considering that MPTMS was successfully grafted onto BC on all cases, the different wetting behavior of modified platforms is associated with the incorporation of polar and nonpolar species produced in the reaction medium onto the surface. The incorporation of those species changes the surface tension, the interfacial tension between liquid and solid. Particularly, the hydrophobic platforms produced by the

**Fig. 4** Contact angle values between a water droplet and the BC-based platforms and their surface tension





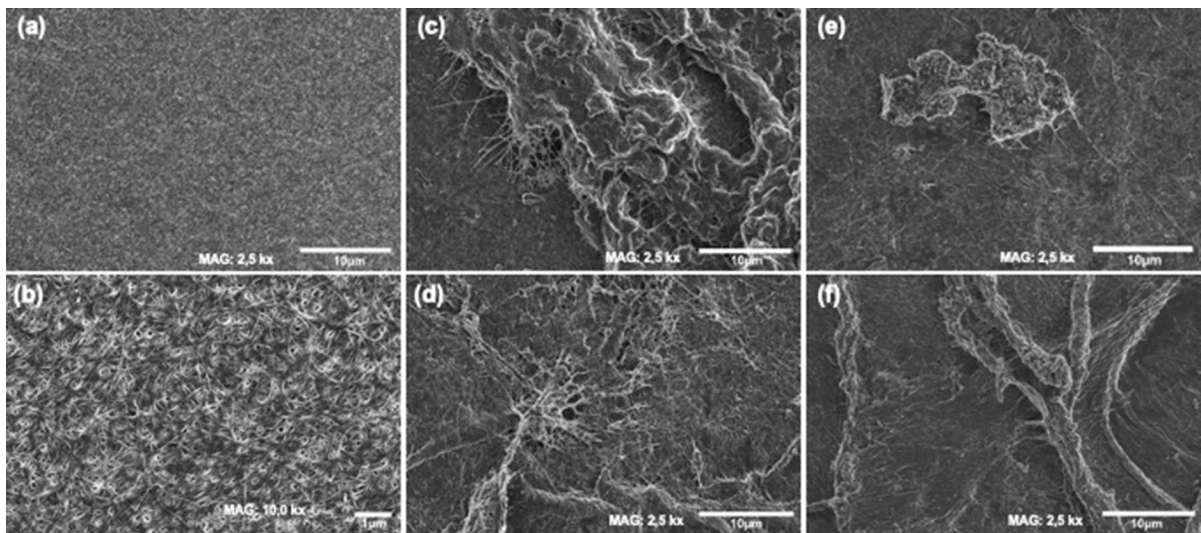
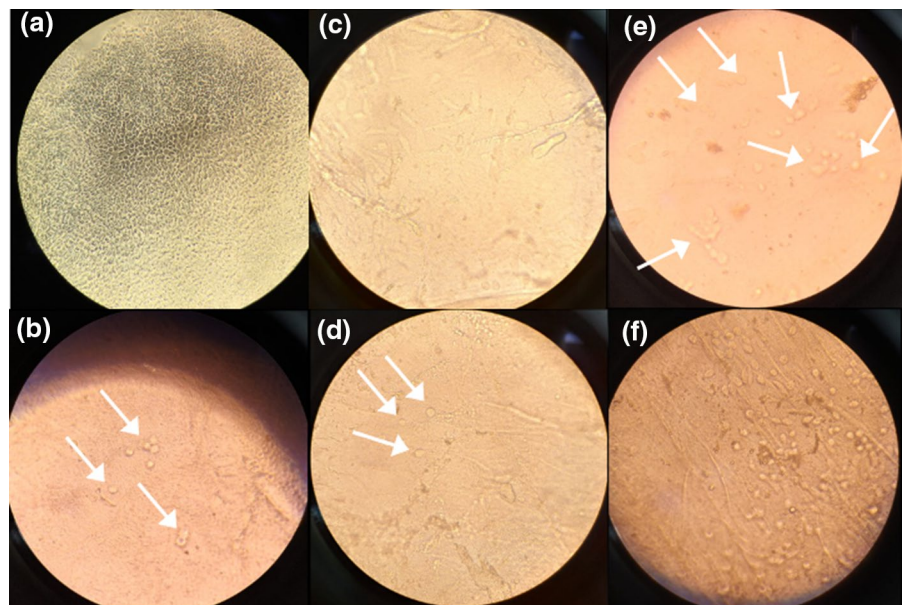


**Fig. 5** FEG-SEM images: (a) and (b) native BC at different magnification, (c) BC-SH CA dried at 28 °C, (d) BC-SH CA dried at 120 °C, (e) BC-SH CB dried at 28 °C, (f) BC-SH CB dried at 120 °C

**Fig. 6** Images viewed by the objective of 40× magnification using an inverted microscope of cells adhered to (a) the bottom of the cell culture well, (b) BC, (c) BC-SH CA dried at 28 °C, (d) BC-SH CA dried at 120 °C, (e) BC-SH CB dried at 28 °C, (f) BC-SH CB dried at 120 °C

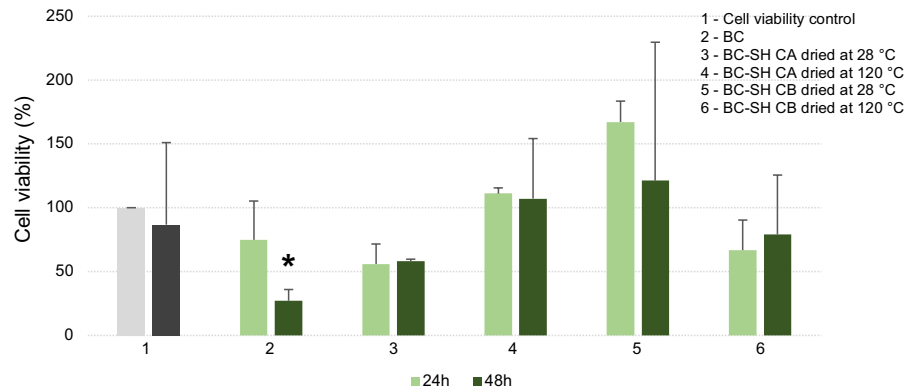


incorporation of nonpolar species under acidic conditions exhibit lower surface tension values while hydrophilic ones incorporated with polar species show higher surface tension values, as seen in Fig. 4.

The results have shown that BC silanization by acid hydrolysis had significantly decreased the substrate polarity while the modification by basic hydrolysis had minor impact on this property. The contact

angle between the solvent droplets and the polymer depends on many factors associated with its surface, including roughness, functional group and surface energy (Gentleman and Gentleman 2014). Considering that the surfaces of the treated BC-based platforms were all functionalized by the insertion of the thiol group, the specific wettability behavior of each material would be the result of two main reasons: by

**Fig. 7** Cell viability graph at 24 and 48 h of cell incubation. Asterisk indicates a statistically significant difference



their surface energy (which proved to be quite different between the platforms treated by acidic and basic hydrolysis), and by their specific fiber rearrangement morphology (see Fig. 5). It is observed that the BC matrix has a distinct three-dimensional structure consisting of an ultra-thin network of cellulose nanofibers, which is ideal for housing cell growth. The surface of the MPTMS-modified platforms is significantly different from the native BC surface in some regions, however the nanometric structure of the fibers was preserved after the chemical treatment.

### Biological assay

Resazurin viability assays were undertaken in treated polystyrene cell culture plates. Wells containing medium and cells were used as control because polystyrene has been employed in the culture of a variety of animal and human cells for over the past 50 years (Lerman et al. 2018). Microscope images in Fig. 6 shows the cells adhered to the bottom of the culture plate and to the surface of the platforms after 48 h of culture incubation. Although fibroblasts had adhered to the materials, those cells have not homogeneously spread along the surfaces.

As revealed from statistical analysis results in Fig. 7, BC-SH CA dried at 120 °C, BC-SH CB dried at 28 °C and BC-SH CB dried at 120 °C exhibited remarkable cell viability (>70%) for both 24 and 48 h of cell incubation. Therefore, those platforms could be considered non-cytotoxic (ISO 10993-5—Biological evaluation of medical devices—Part 5: Tests for in vitro cytotoxicity 2009). Nevertheless, BC achieved non-cytotoxicity according to the regulations only for 24 h of cell cultivation. BC-SH CA

dried at 28 °C have not reach 70% of cell viability in either tested period. Cell growth and proliferation on surfaces are indicative of cytocompatibility, indicating that these materials could be used for biomedical applications (Shao et al. 2017).

Cell viability in the control wells at 24 and 48 h indicates no statistically significant difference, revealing that fibroblasts remained adhered and with active metabolism throughout the experiment. Cell viability associated with control at 24 h was greater than that of BC. Previous studies demonstrate that BC has no cytotoxic effect on a wide variety of cells (Svensson et al. 2005; Czaja et al. 2006; Sanchavanakit et al. 2006), corroborating our results. This result suggests that less cells have adhered to the surface of pristine BC platform compared to the bottom of the culture plate. Furthermore, the mean cell viability of BC at 48 h was lower than at 24 h, with a statistically significant difference between those periods. This may have occurred because fibroblasts have proliferated, forming cell clusters that detached from BC. Similar cell behavior was previously reported by Sanchavanakit et al. (2006). These results indicate that BC is a less favorable support for fibroblast adhesion compared to the traditional cell culture plate. Analogous to BC, the mean cell viability at 24 h for the modified platforms BC-SH CA dried at 28 °C (contact angle = 72.0°) and BC-SH CB dried at 120 °C (contact angle = 29.8°) was lower compared to the control. On the other hand, the mean cell viability at 24 h for BC-SH CA dried at 120 °C (contact angle = 75.8°) and BC-SH CB dried at 28 °C (contact angle = 41.3°) was higher compared to the control on both periods. It reveals that these platforms are suitable support for the adhesion of human fibroblasts.

Is acknowledged that cell adhesion is not only affected by the surface functional group, but also by its density, surface wettability, and cell line (Arima and Iwata 2007). The wettability of a surface is intrinsically linked to its surface energy and roughness. In terms of surface wettability our results corroborate with previous studies which have shown that moderately wettable surfaces that exhibits water contact angles in the range between 40 and 60° facilitates cell adhesion of normal and cancer cell lines (umbilical cord vein endothelial cells and HeLa cells) (Arima and Iwata 2007). On our finds, the BC-based platform with best efficiency of fibroblasts attachment (BC-SH CB dried at 28 °C) was the one that appeared within the range of optimal contact angle according to the literature for this purpose. Lastly, our findings suggest that siloxane-modified BC is a promising support for cell adhesion which might be engineered with regard to the functional group according to the desired properties and the cell line to be cultivated.

## Conclusions

The current study demonstrated simple routes to prepare BC-functionalized siloxanes carrying different functional groups for the purpose of obtaining cellulose-based platforms. Particularly, BC was functionalized with thiol group by using MPTMS under catalytic amounts of acid and base. Although FTIR spectra of the modified platforms were not significantly different from pristine BC, TGA analysis revealed a faster mass loss evolution for the prepared platforms and a higher residue mass associated with the silane grafted onto the cellulosic fibers. This was further certified by elemental analysis which have showed that the sulfur content of the modified platforms originating from the silane was 3–5 times higher than pristine BC. In addition, it was possible to observe in <sup>13</sup>C NMR spectrum of the modified platform the signals associated with both the aliphatic chains inserted onto BC and the methylene carbons of Si–OCH<sub>2</sub>R. Contact angle measurements have shown that surface modification play an important role in the hydrophobicity of BC membranes once those which that underwent acidic conditions have presented a considerable increase on their surface hydrophobicity while the modified platforms produced under basic conditions had maintained its

hydrophilic character. More importantly, the platforms did not show cytotoxicity on normal human lung fibroblasts and have provided good cell attachment, opening new pathways for different strains to be tested for the proposed application. Therefore, our findings suggest that MPTMS-modified BC could be conveniently used as platform for cell culture, contributing towards the development of non-animal testing in many fields of research.

**Funding** This work was funded by São Paulo Research Foundation (FAPESP, Process#2018/23853-2, #2019/12711-5, and #2020/05163-9), National Institute of Photonics (INFo) and Brazilian Higher Education Improvement Coordination (CAPES). We gratefully acknowledge TA Instruments the NEXFILL company from Brazil.

## Declarations

**Competing interests** The authors declare that there is no conflict of interest and that they have no financial interests.

## References

- Arima Y, Iwata H (2007) Effect of wettability and surface functional groups on protein adsorption and cell adhesion using well-defined mixed self-assembled monolayers. *Biomaterials* 28:3074–3082. <https://doi.org/10.1016/j.biomaterials.2007.03.013>
- Beaumont M, Bacher M, Opietnik M et al (2018) A general aqueous silanization protocol to introduce vinyl, mercapto or azido functionalities onto cellulose fibers and nanocelluloses. *Molecules* 23:1427. <https://doi.org/10.3390/molecules23061427>
- Brinker CJ (1988) Hydrolysis and condensation of silicates: effects on structure. *J Non-Cryst Solids* 100:31–50. [https://doi.org/10.1016/0022-3093\(88\)90005-1](https://doi.org/10.1016/0022-3093(88)90005-1)
- Czaja W, Krystynowicz A, Bielecki S et al (2006) Microbial cellulose—the natural power to heal wounds. *Biomaterials* 27:145–151. <https://doi.org/10.1016/j.biomaterials.2005.07.035>
- Daicho K, Fujisawa S, Kobayashi K et al (2020) Cross-polarization dynamics and conformational study of variously sized cellulose crystallites using solid-state <sup>13</sup>C NMR. *J Wood Sci* 66:62. <https://doi.org/10.1186/s10086-020-01909-9>
- de Oliveira Barud HG, Barud HS, Cavicchioli M et al (2015) Preparation and characterization of a bacterial cellulose/silk fibroin sponge scaffold for tissue regeneration. *Carbohydr Polym* 128:41–51. <https://doi.org/10.1016/j.carbpol.2015.04.007>
- de Oliveira Barud HG, da Silva RR, Barud HS et al (2016) A Multipurpose natural and renewable polymer in medical applications: bacterial cellulose. *Carbohydr Polym* 153:406–420. <https://doi.org/10.1016/j.carbpol.2016.07.059>



- De Salvi DTB, Barud HS, Caiut JMA et al (2012) Self-supported bacterial cellulose/boehmite organic–inorganic hybrid films. *J Sol-Gel Sci Technol* 63:211–2018. <https://doi.org/10.1007/s10971-012-2678-x>
- Do Amaral NC, Claro AM, Monteiro GC et al (2019) Surface-modified bacterial cellulose with mercaptosilane as a multifunctional platform. *Int J Adv Med Biotechnol* 2:19–24
- Edmondson R, Broglie JJ, Adcock AF et al (2014) Three-dimensional cell culture systems and their applications in drug discovery and cell-based biosensors. *Assay Drug Dev Technol* 12:207–218. <https://doi.org/10.1089/adt.2014.573>
- Fernandes SCM, Sadocco P, Alonso-Varona A et al (2013) Bioinspired antimicrobial and biocompatible bacterial cellulose membranes obtained by surface functionalization with aminoalkyl groups. *ACS Appl Mater Interfaces* 5:3290–3297. <https://doi.org/10.1021/am400338n>
- Fitaroni LB, de Lima JA, Cruz SA et al (2015) Thermal stability of polypropylene/montmorillonite clay nanocomposites: limitation of the thermogravimetric analysis. *Polym Degrad Stab* 111:102–108. <https://doi.org/10.1016/j.polymdegradstab.2014.10.016>
- Frone AN, Panaitescu DM, Chiulan I et al (2018) Surface treatment of bacterial cellulose in mild, eco-friendly conditions. *Coatings* 8:1–17. <https://doi.org/10.3390/coatings8060221>
- Gentleman MM, Gentleman E (2014) The role of surface free energy in osteoblast–biomaterial interactions. *Int Mater Rev* 59:417–429. <https://doi.org/10.1179/1743280414Y.0000000038>
- Iler RK (1979) *The chemistry of silica: solubility, polymerization, colloid and surface properties, and biochemistry*. New York
- ISO 10993-5 (2009) *Biological evaluation of medical devices - Part 5: tests for in vitro cytotoxicity*
- Kono H, Yunoki S, Shikano T et al (2002) CP/MAS 13C NMR study of cellulose and cellulose derivatives. 1. Complete assignment of The CP/MAS 13C NMR spectrum of the native cellulose. *J Am Chem Soc* 124:7506–7511
- Lantigua D, Kelly YN, Unal B et al (2017) Engineered paper-based cell culture platforms. *Adv Healthc Mater* 6:1–17. <https://doi.org/10.1002/adhm.201700619>
- Lerman MJ, Lembong J, Muramoto S et al (2018) The evolution of polystyrene as a cell culture material. *Tissue Eng Part B Rev* 24:359–372. <https://doi.org/10.1089/ten.teb.2018.0056>
- Lu F, Li H, Sun M et al (2012) Flow injection chemiluminescence sensor based on core–shell magnetic molecularly imprinted nanoparticles for determination of sulfadiazine. *Anal Chim Acta* 718:84–91. <https://doi.org/10.1016/j.aca.2011.12.054>
- Mirbagheri M, Adibnia V, Hughes BR et al (2019) Advanced cell culture platforms: a growing quest for emulating natural tissues. *Mater Horiz* 6:45–71. <https://doi.org/10.1039/c8mh00803e>
- Monteiro AS, Oliveira M, Santagneli S et al (2021) Modification of bacterial cellulose membrane with 1,4-Bis(triethoxysilyl)benzene: a thorough physical–chemical characterization study. *J Phys Chem C* 125:4498–4508
- Ng K, Gao B, Yong KW et al (2016) Paper-based cell culture platform and its emerging biomedical applications. *Mater Today* 00:1–13. <https://doi.org/10.1016/j.mattod.2016.07.001>
- Pagé B, Pagé M, Noel C (1993) A new fluorometric assay for cytotoxicity measurements in vitro. *Int J Oncol* 3:473–476. <https://doi.org/10.3892/ijo.3.3.473>
- Quang Khieu A, Son BHD, Chau VTT et al (2017) 3-Mercaptopropyltrimethoxysilane modified diatomite: preparation and application for voltammetric determination of Lead (II) and Cadmium (II). *J Chem* 2017:1–10. <https://doi.org/10.1155/2017/9560293>
- Robles E, Csóka L, Labidi J (2018) Effect of reaction conditions on the surface modification of cellulose nanofibrils with Aminopropyl Triethoxysilane. *Coatings* 8:139. <https://doi.org/10.3390/coatings8040139>
- Sanchavanakit N, Sangrungrangroj W, Kaomongkolgit R et al (2006) Growth of human keratinocytes and fibroblasts on bacterial cellulose film. *Biotechnol Prog* 22:1194–1199. <https://doi.org/10.1021/bp060035o>
- Shao W, Wu J, Liu H et al (2017) Novel bioactive surface functionalization of bacterial cellulose membrane. *Carbohydr Polym* 178:270–276. <https://doi.org/10.1016/j.carbpol.2017.09.045>
- Svensson A, Nicklasson E, Harrah T et al (2005) Bacterial cellulose as a potential scaffold for tissue engineering of cartilage. *Biomaterials* 26:419–431. <https://doi.org/10.1016/j.biomaterials.2004.02.049>
- Tang W, Jia A, Jia Y et al (2009) The influence of fermentation conditions and post-treatment methods on porosity of bacterial cellulose membrane. *World J Microbiol Biotechnol* 26:125–131. <https://doi.org/10.1007/s11274-009-0151-y>
- Taokaew S, Phisalaphong M, Newby BMZ (2015) Modification of bacterial cellulose with organosilanes to improve attachment and spreading of human fibroblasts. *Cellulose* 22:2311–2324. <https://doi.org/10.1007/s10570-015-0651-x>
- Tibbitt MW, Anseth KS (2009) Hydrogels as extracellular matrix mimics for 3D cell culture. *Biotechnol Bioeng* 103:655–663. <https://doi.org/10.1002/bit.22361>
- Urbina L, Corcuera MA, Gabilondo N et al (2021) A review of bacterial cellulose: sustainable production from agricultural waste and applications in various fields. *Cellulose* 28:8229–8253. <https://doi.org/10.1007/s10570-021-04020-4>
- Wu S (1971) Calculation of interfacial tension in polymer systems. *J Pol Sci C: Pol Symp*. 34:19–30

**Publisher's Note** Springer Nature remains neutral with regard to jurisdictional claims in published maps and institutional affiliations.

Springer Nature or its licensor holds exclusive rights to this article under a publishing agreement with the author(s) or other rightsholder(s); author self-archiving of the accepted manuscript version of this article is solely governed by the terms of such publishing agreement and applicable law.